

OPEN

A pro-oxidant combination of resveratrol and copper down-regulates multiple biological hallmarks of ageing and neurodegeneration in mice

Kavita Pal^{1,2,3}, Gorantla V. Raghuram^{1,2,3}, Jenevieve Dsouza^{1,2}, Sushma Shinde^{1,2}, Vishalkumar Jadhav^{1,2}, Alfina Shaikh^{1,2}, Bhagyeshri Rane^{1,2}, Harshali Tandel^{1,2}, Dipali Kondhalkar^{1,2}, Shahid Chaudhary^{1,2} & Indraneel Mittra^{1,2}

Billions of cells die in the body every day, and cell-free chromatin particles (cfChPs) which are released from them enter into the extracellular compartments of the body, including into the circulation. cfChPs are known to readily enter into healthy cells to damage their DNA and activate apoptotic and inflammatory pathways. We have hypothesized that lifelong assault on healthy cells by cfChPs is the underlying cause of ageing, and that ageing could be retarded by deactivating extra-cellular cfChPs. The latter can be effected by oxygen radicals that are generated upon admixing the nutraceuticals resveratrol and copper (R-Cu). The present study investigated whether prolonged administration of R-Cu would retard biological hallmarks of ageing. C57Bl/6 mice were divided into 3 equal groups; one group was sacrificed at age 3 months, and which acted as young controls. The remaining mice were allowed to age, and at age 10 months the experimental ageing group was given R-Cu by oral gavage twice daily for further 12 months at a dose of 1 mg/kg of R and 0.1 µg/kg of Cu. The control ageing group was given water by oral gavage twice daily for 12 months. Animals of both groups were sacrificed at age 22 months. R-Cu treatment led to reduction of several biological hallmarks of ageing in brain cells which included telomere attrition, amyloid deposition, DNA damage, apoptosis, inflammation, senescence, aneuploidy and mitochondrial dysfunction. R-Cu treatment also led to significant reduction in blood levels of glucose, cholesterol and C-reactive protein. These findings suggest that cfChPs may act as global instigators of ageing and neurodegeneration, and that therapeutic use of R-Cu may help to make healthy ageing an attainable goal.

With progressively increasing longevity, the human race is facing a parallel increase in ageing related degenerative disorders which can severely compromise quality of life. It is predicted that, globally, the number of people age 60 years or above will grow by 38%, from 1 billion to 1.4 billion, outnumbering the youth during the next ten years¹. The United Nations General Assembly has declared 2021–2030 as the Decade of Healthy Ageing, with the ultimate goal to find therapeutic interventions which will simultaneously delay the many conditions associated with ageing^{1,2}. It is argued that healthy ageing should be considered as the ultimate preventive medicine³. Ageing is characterised by a myriad pathological processes which lead to gradual deterioration of structure and function of all cells and tissues of the body⁴, and is associated with a multitude of degenerative disorders such as Alzheimer's disease⁵, cardiovascular diseases⁶, diabetes⁷, and cancer⁸. Although many theories of ageing have been advanced^{9,10}, none can comprehensively explain the numerous changes that accompany this multidimensional process.

DNA damage and chronic inflammation are two cardinal features of ageing^{11,12}. In this context, we have reported that cell-free chromatin particles (cfChPs) that are released from the billions of cells that die in the body

¹Translational Research Laboratory, Tata Memorial Centre, Advanced Centre for Treatment, Research and Education in Cancer, Kharghar, Navi Mumbai 410210, India. ²Homi Bhabha National Institute, Anushakti Nagar, Mumbai 400094, India. ³These authors contributed equally: Kavita Pal and Gorantla V. Raghuram. email: indraneel.mittra@gmail.com

every day, and enter into the extracellular compartments of the body, can be readily internalised by healthy cells wherein they inflict dsDNA breaks, activate apoptotic pathways and induce inflammatory cytokines^{13,14}. This has led us to hypothesise that repeated lifelong assault on healthy cells by cfChPs may be the underlying cause of ageing^{15,16}. Our group has successfully isolated and characterised cfChPs from human serum, which upon EM examination revealed extensive size heterogeneity ranging between ~ 10 and ~ 1000 nm¹³. We have also reported that blood levels of cfChPs increase with age¹⁷.

Our pre-clinical studies have led to the identification of a novel pro-oxidant combination of the nutraceuticals resveratrol (R) and copper (Cu) which deactivates cfChPs via the medium of oxygen radicals^{18–20}. R is a well-known anti-oxidant which has been extensively researched for its health benefits²¹. However, and surprisingly, it acts as a pro-oxidant in presence of Cu, which is also a widely researched nutraceutical²². Fukuhara et al.²³ were the first to report that oxygen radicals are generated when R and Cu are admixed. They showed that R acts as a catalyst to reduce Cu (II) to Cu (I) resulting in generation of oxygen radicals which cleaved plasmid pBR322 DNA²⁴. We have extended these findings to show that a combination of R and Cu can degrade genomic DNA and RNA²⁵, and can deactivate cfChPs in vivo by degrading their DNA component^{18–20,25}. We have further observed that, paradoxically, the DNA degrading activity of R–Cu increases as the molar concentration of Cu is gradually reduced with respect to R²⁵. On the basis of this finding, in the present study, we kept the molar ratio of R:Cu at 1:10⁴.

We have reported that a combination of R and Cu, when used at a molar ratio of 1:10⁴, has therapeutic effects in several pre-clinical conditions associated with elevated extracellular levels of cfChPs^{18–20}. For example, orally administered R–Cu can ameliorate toxic side effects of chemotherapy¹⁸, and radiation therapy¹⁹, and prevent bacterial endotoxin induced cytokine storm and fatality in mice²⁰. Our early results also suggest that R–Cu is therapeutically effective in humans. An observational study showed that orally administered R–Cu to patients with severe Covid-19 led to reduction in mortality by nearly 50%²⁶. We have also reported that grade III–IV mucositis could be significantly reduced by orally administered R–Cu in patients receiving high dose chemotherapy and bone marrow transplant for multiple myeloma²⁷. R–Cu treatment also led to significant reduction in blood levels of inflammatory cytokines in that study.

Oxygen radicals that are generated upon oral administration of R–Cu are apparently absorbed from the stomach to have systemic effects in the form of deactivation/eradication of extracellular cfChPs^{18–20,26,27}. In the present study, we have taken advantage of cfChPs deactivating property of R–Cu to investigate whether prolonged administration of R–Cu to ageing mice will retard the hallmarks of ageing and neurodegeneration. The dose of R used in our study was 1 mg/kg, and that of Cu was 0.1 µg/kg, given by oral gavage twice daily. This dose of Cu was 20,000 times less, and that of R 5 times less, than those that have been used in pre-clinical studies to investigate their health promoting properties by other investigators^{28,29}.

Using confocal microscopy and antibodies against DNA and histone we detected copious presence of extracellular cfChPs in brain of ageing mice, and observed that cfChPs were deactivated/eradicated following prolonged oral administration of R–Cu. Deactivation/eradication of cfChPs was associated with down-regulation of multiple biological hallmarks of ageing in brain cells. At a systemic level, R–Cu treatment led to significant reduction in blood levels of glucose, cholesterol and C-reactive protein. Taken together, our results suggest that cfChPs act as global instigators of ageing and neurodegeneration, and that therapeutic use of R–Cu may help to make healthy ageing an attainable goal.

Methods

Animal ethics approval. The experimental protocol of this study was approved by the Institutional Animal Ethics Committee (IAEC) of Advanced Centre for Treatment, Research and Education in Cancer (ACTREC), Tata Memorial Centre, Navi Mumbai, India under permission No.16/2015. The experiments were carried out in compliance with the IAEC animal safety guidelines, and with those of ARRIVE guidelines.

ACTREC- IAEC maintains respectful treatment, care and use of animals in scientific research. It aims that the use of animals in research contributes to the advancement of knowledge following the ethical and scientific necessities. All scientists and technicians involved in this study have undergone training in ethical handling and management of animals under supervision of FELASA certified attending veterinarian. Animals were euthanised at appropriate time points under CO₂ atmosphere by cervical dislocation under supervision of FELASA trained animal facility personnel.

Source of resveratrol and copper. The sources of R and Cu were: Resveratrol (Trade name—Trans-MaxTR, Biotivia LLC, USA (<https://www.biotivia.com/product/transmax/>)); Copper (Trade name—Chelated Copper, J.R. Carlson Laboratories Inc. USA (<https://carlsonlabs.com/chelated-copper/>)).

Animals and R–Cu dosing. Inbred C57Bl/6 mice obtained from the Institutional Animal Facility were maintained following our Institutional Animal Ethics Committee standards. They were housed in pathogen-free cages containing husk bedding under 12-h light/dark cycle with free access to water and food. The HVAC system was used to provide controlled room temperature, humidity and air pressure.

The study comprised of 24 C57Bl/6 mice, 12 of which were male and 12 were female. Four mice of either sex were sacrificed when they were 3 months old, and acted as young controls. The remaining 16 mice (8 male and 8 female) were allowed to age until they were 10 months old and divided into two groups: (1) Ageing control mice (N = 4 of each sex), and (2) R–Cu treated ageing mice (N = 4 of each sex). Animals of both groups were sacrificed after 12 months when they were 22 months old.

R–Cu was administered twice daily by oral gavage for 12 months (from 10 to 22 months) at a dose of 1 mg/kg of R and 0.1 µg/kg of Cu. R, being insoluble in water, was administered as water suspension (100 µL), and Cu

was administered as a water-based solution (100 μ L). The ageing control mice were given water (100 μ L) twice daily by oral gavage. Our previous studies have shown this dose of R-Cu is therapeutically effective in multiple other pre-clinical conditions¹⁸⁻²⁰.

Reduced physical activity and weight loss of mice were used as humane endpoints of the study and were scored twice every week. At appropriate time points as indicated above, blood was collected via retro-orbital route under isoflurane anaesthesia for serum separation. Animals were then euthanised under CO₂ atmosphere by cervical dislocation under supervision of FELASA trained animal facility personnel. After euthanasia, brain was harvested from all animals, fixed in 10% formalin and paraffin blocks were prepared for further analysis.

Reagents, antibodies and kits. Details of commercial sources and catalogue numbers of reagents, antibodies and analytical kits used in this study are given in supplementary table 1.

Assessment of superoxide Dismutase (SOD) levels in brains cells. Expression of SOD in brain cells was estimated using immunofluorescence (IF) technique as described by us earlier^{18,20}. Briefly, FFPE sections were deparaffinised, rehydrated in alcohol series, incubated in 0.01 M citrate buffer (pH 6.0) at 95 °C for 20 min and washed in 1X PBS. Sections were immune-stained using primary antibody against SOD and corresponding secondary antibody (Suppl. Table 1). Images were acquired and analysed using FISH view software version 8.1 (<https://spectral-imaging.com>, Applied Spectral Imaging, Israel).

Superoxide Dismutase (SOD) activity in serum. Serum SOD activity was measured by ELISA using a commercial kit (Cell Biolabs, CA, USA; cat no # STA 340) according to manufacturer's instructions.

Detection of cfChPs in extra-cellular spaces of brain by fluorescence immune-staining and confocal microscopy. Immune-staining for DNA and histone H4 followed by confocal microscopy was performed on formalin fixed paraffin embedded (FFPE) sections of brain as described in detail by us earlier²⁰. Fluorescence intensity of five randomly chosen confocal fields (~ 50 cells in each field) was recorded, and mean fluorescence intensity (MFI) (\pm S.E.M) was estimated.

Assessment of telomere abnormalities. *Telomere length estimation by qRT-PCR.* The average telomere length from the brain tissue was estimated using a highly sensitive quantitative real-time PCR (qRT-PCR) technique^{30,31}. Genomic DNA was isolated from brain tissue using DNeasy blood & Tissue Kit (Qiagen, Hilden, Germany). DNA quantification was performed using a Nanodrop™ spectrophotometer (Thermo Fisher Scientific, Waltham, USA). Ten nanogram of DNA was used in 5 μ L of 1 \times SYBR Select Master Mix (Applied Biosystems, Foster City, CA, USA), 250 nM of both telomere specific primers or 350 nM of 36B4 primers to a total volume of 10 μ L reactions. The thermal cycling conditions for both Telomere and 36B4 are: initial denaturation of 95 °C for 10 min followed by 40 cycles of 95 °C for 15 s, 60 °C for 30 s & 72 °C for 30 s. The sequence for telomere-specific forward and reverse primers (Sigma-Aldrich) are 5' CGG TTT GTT TGG GTT TGG GTT TGG GTT TGG GTT TGG GTT 3' & 5' GGC TTG CCT TAC CCT TAC CCT TAC CCT TAC CCT TAC CCT 3'. The sequences for acidic ribosomal phosphoprotein (36B4)—specific forward and reverse primers are 5' ACT GGT CTA GGA CCC GAG AAG 3' and 5'TCA ATG GTG CCT CTG GAG ATT 3', respectively). Genomic DNA isolated from the spleen of an individual mouse was used as a reference DNA and serially diluted for telomere and 36B4 PCR. All samples were assayed in duplicate on a QuantStudio™ 12 K Flex Real-Time PCR System (ThermoFisher) using 384-well block. Standard curves were generated and the relative input amount for both telomere and 36B4 were calculated. The average of the ratio of telomere and 36B4 was reported as the average telomere length.

Telomere Q-FISH. Quantitative telomere FISH was performed using Cy3-labeled peptide nucleic acid (PNA) telomere probes (supplementary table 1). FFPE sections of brain were de-paraffinized and serially dehydrated in absolute ethanol series (70/80/100%) followed by antigen retrieval in sodium citrate buffer (pH 6) at 90 °C in water bath and cooled to room temperature. Sections were dehydrated in alcohol series and denatured at 75 °C for 6 min. Sections were then hybridised with PNA telomere probes overnight at 37 °C. Unbound probes were washed with 2X saline sodium citrate (SSC) buffer followed by 4X SSC at 56 °C for 3 min each. The sections were finally washed in 4X saline sodium citrate Tween-20 (SSCT) buffer at room temperature and mounted in VectaShield DAPI. Images were acquired and analysed using Applied Spectral Bio-imaging system (Applied Spectral Imaging, Israel). Images of ~ 500 interphase nuclei were acquired using SpotScan Software 8.1 (<https://spectral-imaging.com>, Applied Spectral Imaging, Israel) in a multichannel 3-D mode with a constant exposure of 1000 ms for Cy3 (telomeres) and 150 ms for DAPI (nuclei) throughout the experiments. Each 3D image comprised of a stack of 11 focal planes per cell with a sampling distance of 500 nm along the z direction and 107 nm in the xy direction. Images were de-convoluted and telomere numbers per nucleus was estimated using Spot Count algorithm in SpotView software 8.1 (<https://spectral-imaging.com>, Applied Spectral Imaging, Israel). Number of telomere aggregates per nucleus was estimated visually.

Assessment of β - amyloid deposition in brain and BDNF in serum. Detection of amyloid deposition in brain was examined by confocal microscopy on FFPE sections following fluorescent-immune staining using primary antibody against β -amyloid and an appropriate secondary antibody (supplementary table 1). Serum BDNF was estimated by ELISA using a commercial kit (supplementary table 1) according to manufacturer's instructions.

Assessment of DNA damage, apoptosis and Inflammation in brain cells. γ -H2AX, active caspase-3 and NF- κ B expression were analysed on FFPE sections of brain tissue by standard IF method using appropriate antibodies (supplementary table 1) as described by us earlier^{18,20}.

Assessment of senescence in brain cells. Assessment of biomarkers of senescence was performed on FFPE sections of brain tissue which included: (1) co-localisation of telomere and γ -H2AX IF signals using Immuno-FISH; (2) co-localization of 53BP1 and pro-myelocytic leukemia-nuclear bodies (PML-NBs) IF signals; (3) p16^{INK4a} expression by IF using appropriate antibodies.

Assessment of aneuploidy in brain cells. Aneuploidy was assessed with respect to chromosome numbers 7 and 16 by FISH using chromosome specific probes on FFPE sections of brain tissues. Sections were deparaffinised and dehydrated in alcohol series (70–100%) followed by antigen retrieval in sodium citrate buffer (pH 6) at 90 °C in water bath and then cooled to room temperature. Sections were hybridised with chromosome 7 and 16 specific DNA probes overnight at 37 °C. Unbound probes were washed off with 2X SSC followed by 0.4X SSC at 70 °C for 3 min each. The sections were finally washed in 4X SSCT and mounted in VectaShield DAPI. Images were acquired and analysed using Applied Spectral Bio-imaging system (Applied Spectral Imaging, Israel). Number of fluorescent signals per nucleus was counted, and signals more or less than 2 N were considered as evidence of aneuploidy. Five fields containing ~ 500 nuclei were analysed and average number of signals per nucleus was calculated.

Assessment of mitochondrial dysfunction in brain cells. Mitochondrial dysfunction was analysed by IF on FFPE sections of brain tissue to assess the expression of the mitochondrial trans-membrane protein TOMM20. Estimation of volumetric changes in TOMM20 expression was performed using IMARIS software 7.2.3 (<http://www.bitplane.com>, Bitplane Technologies, AG). Mean volume (in x–y–z planes) was calculated for 5 images (> 2,000 mitochondria) for each brain section.

Assessment of systemic metabolic dysfunction. Serum glucose and cholesterol levels were estimated using an automated instrument (Dimension EXL with LM, Siemens). Serum C-reactive protein (CRP) levels were measured using a commercial ELISA kit (supplementary table 1) as per the manufacturer's protocol.

Statistical analysis. Statistical analyses were performed using GraphPad Prism 6.0 (<https://www.graphpad.com/>, GraphPad Software, Inc., USA). The results of aged control mice were compared with young controls and aged + R–Cu treated mice. Mean (\pm SEM) values for four mice in each group for both sexes were compared using non-parametric unpaired student's t test, separately for both sexes.

Ethical approval. The study was approved by the Institutional Animal Ethics Committee (IAEC) of Advanced Centre for Treatment, Research and Education in Cancer (ACTREC). ACTREC IAEC adheres to ARRIVE guidelines. The experiments in this study were undertaken in compliance with ARRIVE guidelines (supplementary table 2).

Results

R–Cu up-regulates SOD in brain cells and increases SOD activity in serum. As a first step, we investigated whether oral R–Cu treatment might have led to generation of free-radicals in the brain. As expected, ageing mice showed significant reduction in SOD levels in brain cells ($p < 0.05$ and $p < 0.01$ in female and male mice, respectively) (Fig. 1). However, R–Cu treatment led to marked increase in SOD levels that were similar to that detected in young control mice ($p < 0.01$ in both female and male mice) (Fig. 1). This finding suggested that oxygen radicals were apparently being generated in vivo following R–Cu treatment, and that they appeared to have entered into brains cells. The latter in an attempt to eliminate the invading oxygen radicals had activated an anti-oxidant defence mechanism by up-regulating the anti-oxidant enzyme SOD. It should be noted however that the IF method that we used to detect SOD expression in brain cells does not reflect its biological activity. However, R–Cu treatment did lead to an increase in SOD activity in serum of ageing mice, restoring them to levels similar to those seen in young control mice ($p < 0.01$ and $p < 0.05$ in female and male mice, respectively) (Supplementary Figure S1). Based on the increased SOD activity in serum in R–Cu treated mice, it can be assumed that SOD activity had also increased in brain cells.

Detection of copious presence of cfChPs in extra- cellular spaces of ageing brain and their deactivation/eradication by R–Cu. Confocal microscopy of FFPE sections of ageing mouse brain was performed following fluorescent immuno-staining with anti-DNA (red) and anti-histone (green) antibodies. Upon superimposing DNA and histone fluorescent images, copious presence of cfChPs (yellow fluorescent signals) were detected in the extracellular spaces of brain of ageing mice (Fig. 2). cfChPs were virtually eliminated following R–Cu treatment for one-year. This finding indirectly suggested, that oxygen radicals generated in the mouse brain had apparently deactivated/eradicated the profusion of cfChPs that were present in the extra-cellular spaces of ageing mouse brain. It should be noted from Fig. 2 that not all red (DNA) and green (histone) fluorescent signals had strictly co-localised. This may have resulted from unevenness of cut surfaces of FFPE sections which prevented the respective antibodies to access the DNA and Histone epitopes on cfChPs. Quantification of MFI of yellow fluorescent cfChPs signals showed a remarkable reduction in cfChPs in extracellular spaces of ageing brain following one-year treatment with R–Cu ($p < 0.01$ in both sexes) (Fig. 2).

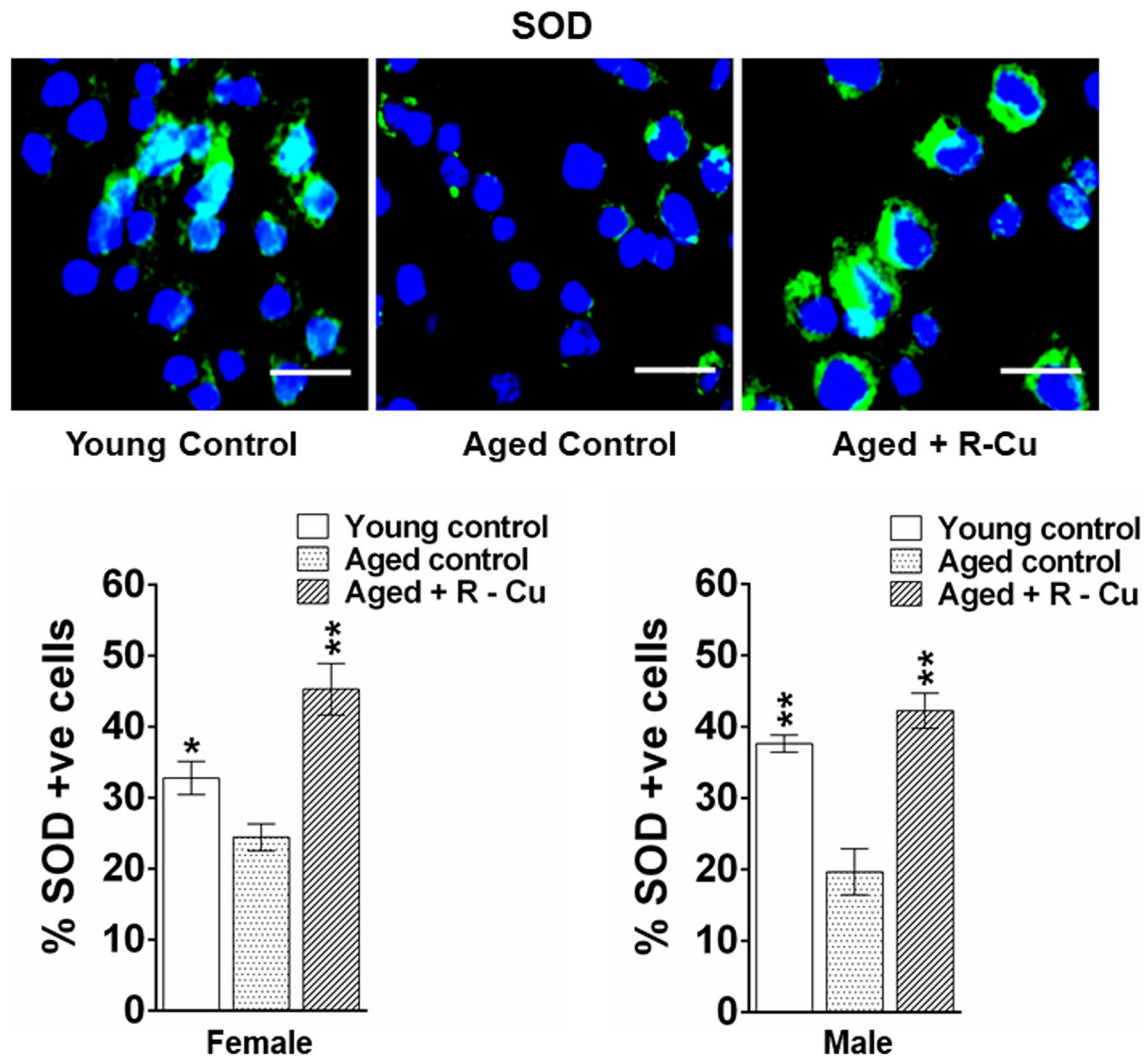


Figure 1. Loss of SOD activity in brain cells of ageing mice and its restoration by R-Cu treatment. Representative IF images of SOD expression in brain cells (upper panel) (Scale bar = 10 μ m), and quantification of SOD levels expressed as histograms (lower panel). For each slide 1000 cells were analysed and percent cells positive for SOD were calculated. Bars represent mean \pm SEM values. N = 4 animals in each group of both sexes. Values of young control mice and R-Cu treated ageing mice were compared with those of ageing control mice, and statistical analysis was performed by two-tailed Student's t test. * p < 0.05; ** p < 0.01.

R-Cu reduces telomere abnormalities in ageing brain cells. Telomeres play a central role in cellular changes associated with ageing³². Telomere attrition, telomere loss and telomere aggregation are cardinal features of ageing^{32,33}. We estimated telomere length in brain cells by qRT-PCR and observed a significant reduction in telomere length in mice of both sexes (p < 0.0001 and p < 0.01 in female and male mice, respectively) (Fig. 3A). R-Cu treatment restored telomere length to a significant degree in female mice (p < 0.001), but not in male mice (Fig. 3A). With respect to number of telomere signals per brain cell, a reduction was seen in ageing mice of both sexes (p < 0.01 in both sexes), which was again significantly restored following R-Cu treatment in female (p < 0.01) but not in male mice (Fig. 3B,C). A similar observation was made with respect to aggregation of telomeres, which was significantly increased in ageing mice of both sexes (p < 0.001 and p < 0.01 in female and male mice, respectively), but was significantly reduced following R-Cu treatment only in female mice (p < 0.01) (Fig. 3B,D). Thus, overall, with respect to telomere abnormalities, R-Cu was found to be effective in restoring telomere abnormalities in female but not in male mice.

R-Cu reduces amyloid deposition in ageing brain and restores of BDNF levels in serum. Increased amyloid (A β) protein deposition in extra-cellular spaces of brain cells is classically associated with Alzheimer's disease^{34,35}. Confocal microscopy using antibody against β -amyloid detected markedly increased amyloid deposition in the form of amyloid fibrils in ageing mice. The latter was remarkably reduced following one year of R-Cu treatment (Fig. 4A, left hand panel). Quantification of MFI confirmed the marked increase in extracellular β -amyloid deposition in ageing mice brain (p < 0.0001 and p < 0.01 in female and male

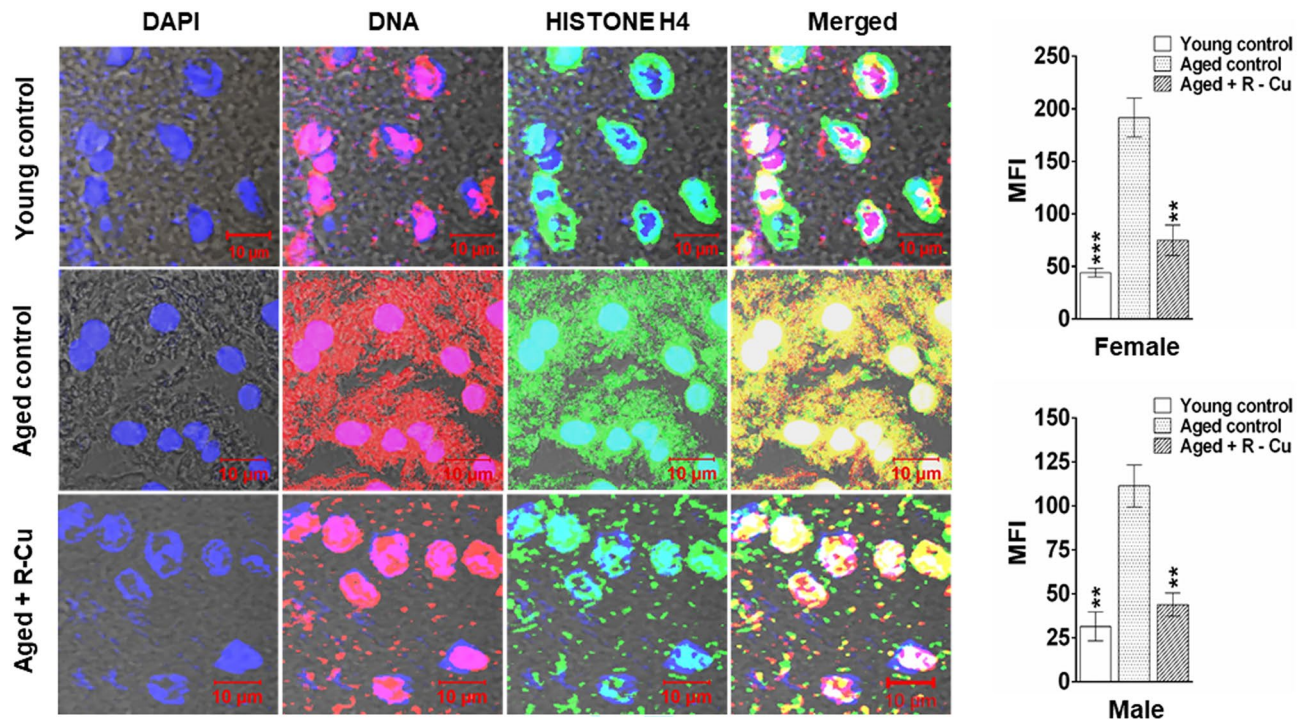


Figure 2. Copious presence of cfChPs in extra- cellular spaces of ageing brain and their deactivation/ eradication by R-Cu treatment. Representative confocal images of FFPE sections following fluorescent immunostaining with anti-DNA (Red) and anti-histone antibodies, showing co-localization of red and green signals to generate yellow/white coloured particles which represent cfChPs (left hand panel). Quantification of yellow IF signals expressed as histograms (right hand panel). Fluorescence intensity of five randomly chosen confocal fields (~ 50 cells in each field) from each section was recorded. Bars represent mean \pm SEM values. N = 4 animals in each group of both sexes. Values of young control mice and R-Cu treated ageing mice were compared with those of ageing control mice, and statistical analysis was performed by two-tailed Student's t test. ** $p < 0.01$, *** $p < 0.001$.

mice, respectively). One year of R-Cu treatment resulted in significant reduction in extra-cellular amyloid in mice of both sexes ($p < 0.01$ and $p < 0.5$ in female and male mice, respectively) (Fig. 4A, right hand panel).

Brain derived neurotrophic factor (BDNF), which plays an important role in neuronal survival and growth³⁶, was greatly reduced in sera of ageing mice of both sexes as measured by ELISA ($p < 0.01$ and $p < 0.05$ in female and male mice, respectively) (Fig. 4B). R-Cu treatment for one year resorted serum BDNF levels nearly to those seen in young mice in both sexes ($p < 0.05$ and $p < 0.001$ in female and male mice, respectively) (Fig. 4B).

R-Cu reduces DNA damage, apoptosis and inflammation in ageing brain cells. We next examined several other hallmarks of ageing viz. DNA damage, apoptosis and inflammation in brain cells^{37–39}. DNA damage was examined using phosphorylation of H2AX as a marker of dsDNA breaks⁴⁰. γ -H2AX levels were markedly increased in ageing mice ($p < 0.001$ and $p < 0.0001$ in female and male mice, respectively). R-Cu treatment reduced γ -H2AX levels ($p < 0.01$ and $p < 0.05$ in female and male mice, respectively) (Fig. 5A, left & right hand panels).

We next examined active caspase-3 levels, which is known to be a marker of mitochondria mediated apoptosis⁴¹. Highly significant increase in apoptosis in ageing brain cells was seen in both sexes ($p < 0.0001$). R-Cu treatment significantly reduced the degree of apoptosis in mice of both sexes ($p < 0.01$ and $p < 0.0001$ in female and male mice, respectively) (Fig. 5B, left & right hand panels).

Inflammation is a cardinal hallmark of ageing¹², and we assessed the expression of the transcription factor NF- κ B in brain cells. The latter was highly significantly elevated in ageing mice of both sexes ($p < 0.0001$). R-Cu treatment significantly reduced NF- κ B levels in both sexes ($p < 0.05$ and $p < 0.01$ in female and male mice, respectively) (Fig. 5C, left & right hand panels).

R-Cu reduces senescence in ageing brain cells. Senescence is the hallmark of biological ageing characterised by gradual deterioration of cellular functions⁴². We observed persistence of numerous co-localizing signals of γ -H2AX with those of telomeres (DNA-SCARS)—a classical hallmark of senescence⁴³—in ageing mice of both sexes ($p < 0.001$). Quantification of co-localising signals revealed a marked reduction following R-Cu treatment ($p < 0.01$ in both sexes) (Fig. 6A, upper & lower panels).

Double strand DNA breaks form a storage hub for several heterochromatin-binding proteins in the form of senescence-associated heterochromatic foci (SAHF)⁴⁴. One such heterochromatin binding protein is

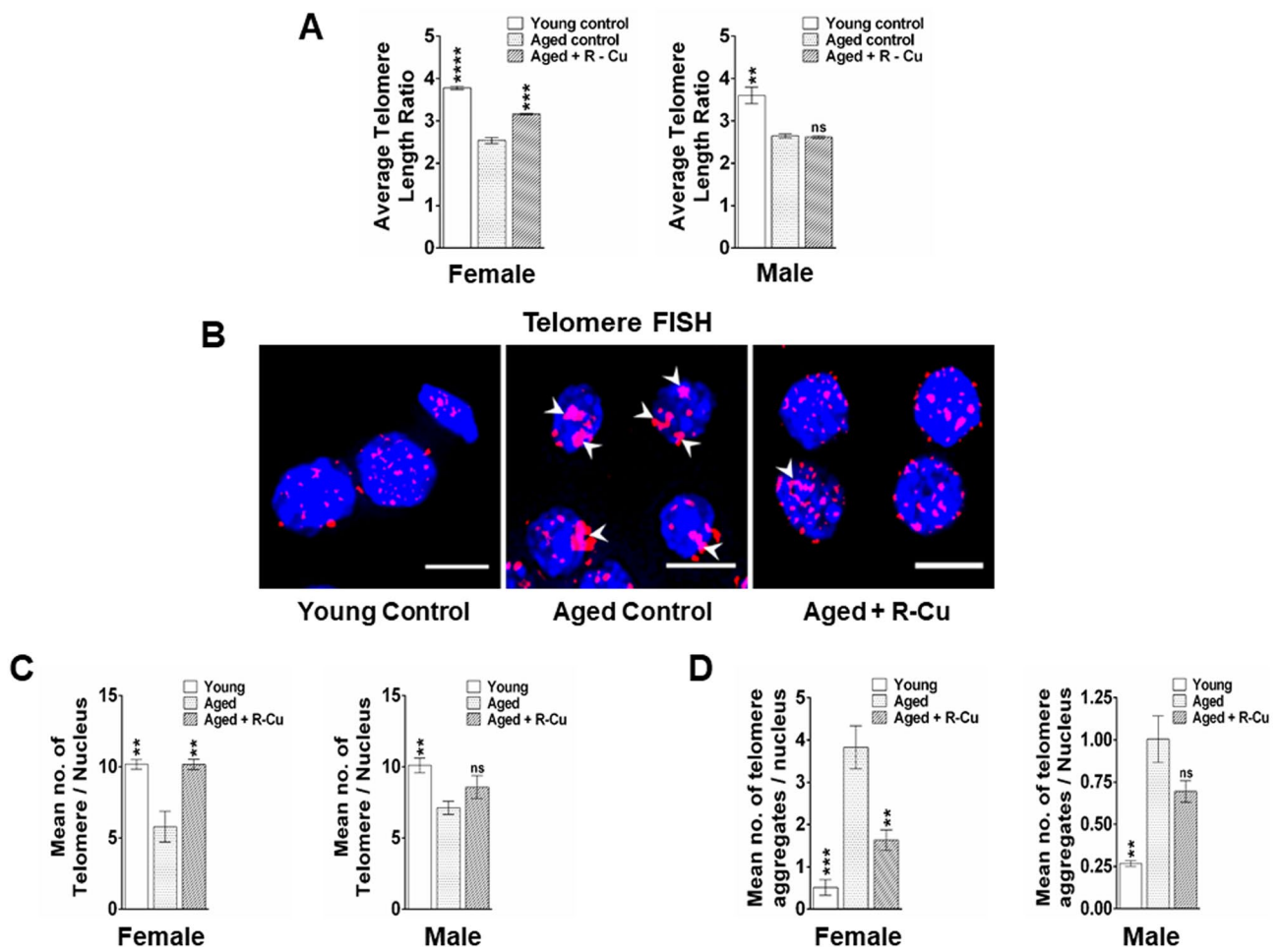


Figure 3. Telomere abnormalities in brain cells of ageing mice and their prevention by treatment with R-Cu. (A) Estimation of telomere length by quantitative RT-PCR. Bars represent mean \pm SEM values. N = 4 animals of both sexes, except in R-Cu treated female mice wherein N was 3; (B) Representative images of telomere FISH (Scale bar = 10 μ m). (C) Histograms representing number of telomeres per nucleus as estimated by SpotScan Software 8.1 (<https://spectral-imaging.com>, Applied Spectral Imaging, Israel). Mean number of fluorescent telomere signals per nucleus from five randomly chosen fields (~ 500 nuclei) is represented in the histograms. Bars represent mean \pm SEM values. N = 4 animals each group of both sexes; (D) Histograms representing telomere aggregates per nucleus (marked by arrow heads in B). Mean number of fluorescent telomere aggregates per nucleus from five randomly chosen fields (~ 500 nuclei) is represented in the histograms. Bars represent mean \pm SEM values. N = 4 animals each group of both sexes. In (A,C,D) values in young controls and R-Cu treated ageing mice were compared with those of ageing controls, and statistical analysis was performed by two-tailed Student's t test. ** p < 0.01; *** p < 0.001; **** p < 0.0001.

pro-myelocytic leukemia-nuclear bodies (PML-NBs) which has been shown to be significantly correlated with DNA damage associated senescence in ageing mice^{45,46}. We show that the number of co-localizing signals of 53BP1 and PML were markedly increased in ageing mice of both sexes (p < 0.0001). Co-localising signals were significantly reduced following R-Cu treatment for 1 year (p < 0.05 and p < 0.01 in female and male mice, respectively) (Fig. 6B, left & right hand panels).

Another marker of senescence that we examined was p16^{INK4a}⁴⁷, which was elevated in ageing mice of both sexes (p < 0.0001 for both sexes). R-Cu treatment significantly reduced levels of p16^{INK4a} (p < 0.05 and p < 0.01 in female and male mice, respectively) (Fig. 6C, upper & lower panels).

R-Cu reduces aneuploidy in ageing brain cells. Telomere loss resulting in fusion of chromosomes in ageing mice can cause aneuploidy resulting in abnormal number of chromosomes⁴⁸. We examined the degree of aneuploidy in brain cells with respect to chromosome no 7 and 16, and observed a ~ 15 fold increase in aneuploidy in ageing mice with respect to both chromosomes (p < 0.0001 for both chromosomes in both sexes) (Fig. 7, left & right hand panels). R-Cu treatment markedly reduced aneuploidy with respect to both chromosomes in both sexes (p < 0.001) (Fig. 7, left & right hand panels).

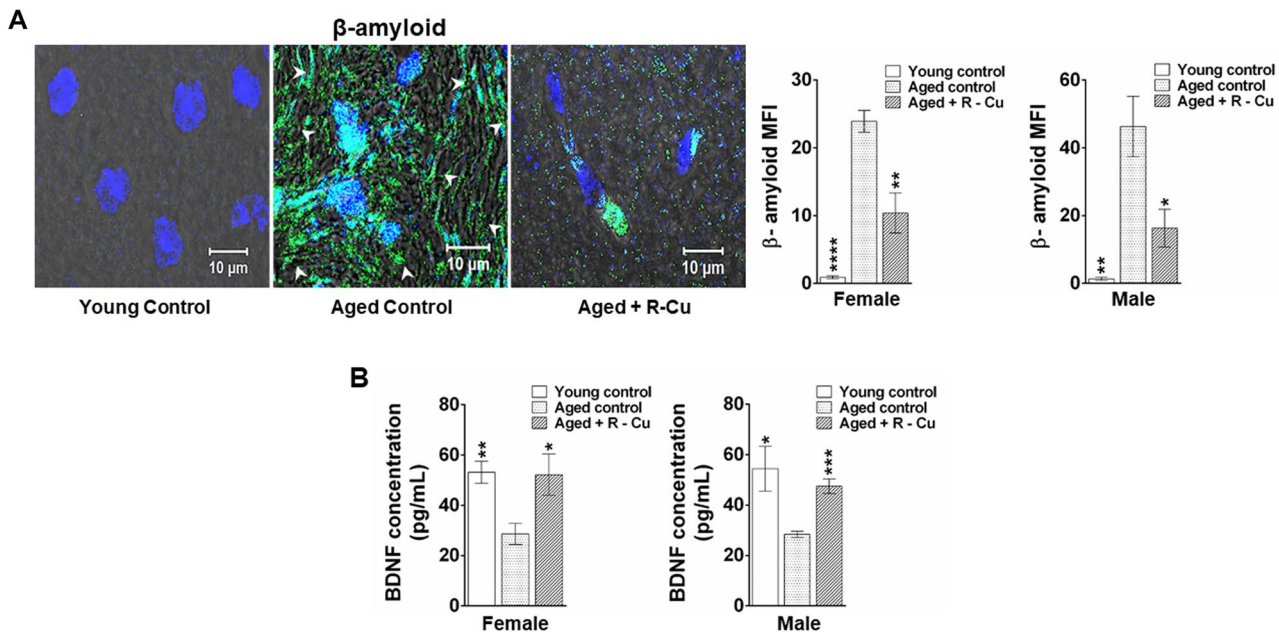


Figure 4. Increased β -amyloid deposition in ageing brain and reduced BDNF in serum, both of which are reversed by treatment with R-Cu. (A) Representative confocal images of β -amyloid deposition in brain as detected by IF (left hand panel). Quantitative histograms representing mean MFI values (\pm SEM) of β -amyloid fluorescence (right hand panel). For each slide, brain area covered by 1000 cells were analysed. N = 4 animals in each group of both sexes. (B) Quantitative histograms representing mean serum BDNF levels (\pm SEM). N = 4 animals in each group of both sexes except, young control female (N = 3), ageing R-Cu treated female (N = 3), and ageing control male mice (N = 3). In both (A) and (B), values in young controls and R-Cu treated ageing animals were compared with those of ageing controls, and statistical analysis was performed by two-tailed Student's t test. * p < 0.05; ** p < 0.01; *** p < 0.001; **** p < 0.0001.

R-Cu reduces mitochondrial dysfunction in ageing brain cells. Mitochondrial DNA integrity and functionality decrease with age resulting in accumulation of oxidative damage caused by reactive oxygen species (ROS)⁴⁹. We studied mitochondrial dysfunction by analysing the expression of TOMM20, a nuclear-encoded subunit of the mitochondrial translocation complex which imports other nuclear-encoded proteins. Its overexpression is reported to promote neurodegeneration⁵⁰. Our results revealed overexpression of TOMM20 on mitochondrial membrane leading to increase in total mitochondrial volume in ageing brain cells when compared to young controls ($p < 0.001$ in both sexes). R-Cu treatment significantly restored mitochondrial volume ($p < 0.05$ and $p < 0.01$ in female and male mice, respectively) (Fig. 8, upper & lower panels).

R-Cu reduces systemic metabolic dysfunction in ageing mice. Metabolic ageing involves dysregulation of physiological processes leading to insulin resistance and lipid accumulation brought about by low grade chronic inflammation^{51,52}. As anticipated serum glucose levels was significantly elevated in ageing mice⁵³ ($p < 0.01$ for both sexes), which was reduced to levels seen in young controls following one-year treatment with R-Cu ($p < 0.01$ for both sexes) (Fig. 9A). Serum cholesterol was significantly elevated in ageing female mice ($p < 0.05$) but not in male mice (Fig. 9B). Serum cholesterol was significantly elevated in ageing female mice ($p < 0.05$) but not in male mice (Fig. 9B). Nonetheless, R-Cu treatment significantly reduced serum cholesterol levels in both sexes ($p < 0.001$ and $p < 0.05$ in female and male mice, respectively). CRP was highly significantly elevated in ageing mice of both sexes ($p < 0.0001$) and was reduced by R-Cu treatment ($p < 0.05$ in both sexes) (Fig. 9C).

Discussion

ROS are short lived molecular species containing an unpaired electron which makes them highly reactive as they search for another electron to pair with, and in the process can damage biomolecules such as DNA, proteins and lipids⁵⁴. ROS induced oxidative stress is known to have multiple deleterious effects on host cells⁵⁵. However, we have reported that, paradoxically, when ROS is artificially generated outside the cell in the extracellular spaces of the body, they can have wide ranging therapeutic effects^{18–20,26,27}. Admixing R with Cu leads to generation of oxygen radicals by virtue of the ability of R to reduce Cu (II) to Cu (I)^{23,25}. Oxygen radicals that are generated in the stomach upon oral administration of R-Cu are apparently absorbed to have systemic effects in the form of deactivation/eradication of extracellular cfChPs. We have shown that cfChPs have wide-ranging damaging effects on host cells. For example, cfChPs can readily enter into the healthy cells to damage their DNA, activate inflammatory cytokines and promote apoptosis via the mitochondrial pathway^{13,14}. Given that 1×10^9 – 1×10^{12} cells die in the body every day^{56,57}, we have hypothesised that repeated and lifelong assault on healthy cells by cfChPs derived from the dying cells may be the underlying cause of ageing^{15,16}. In support of this hypothesis

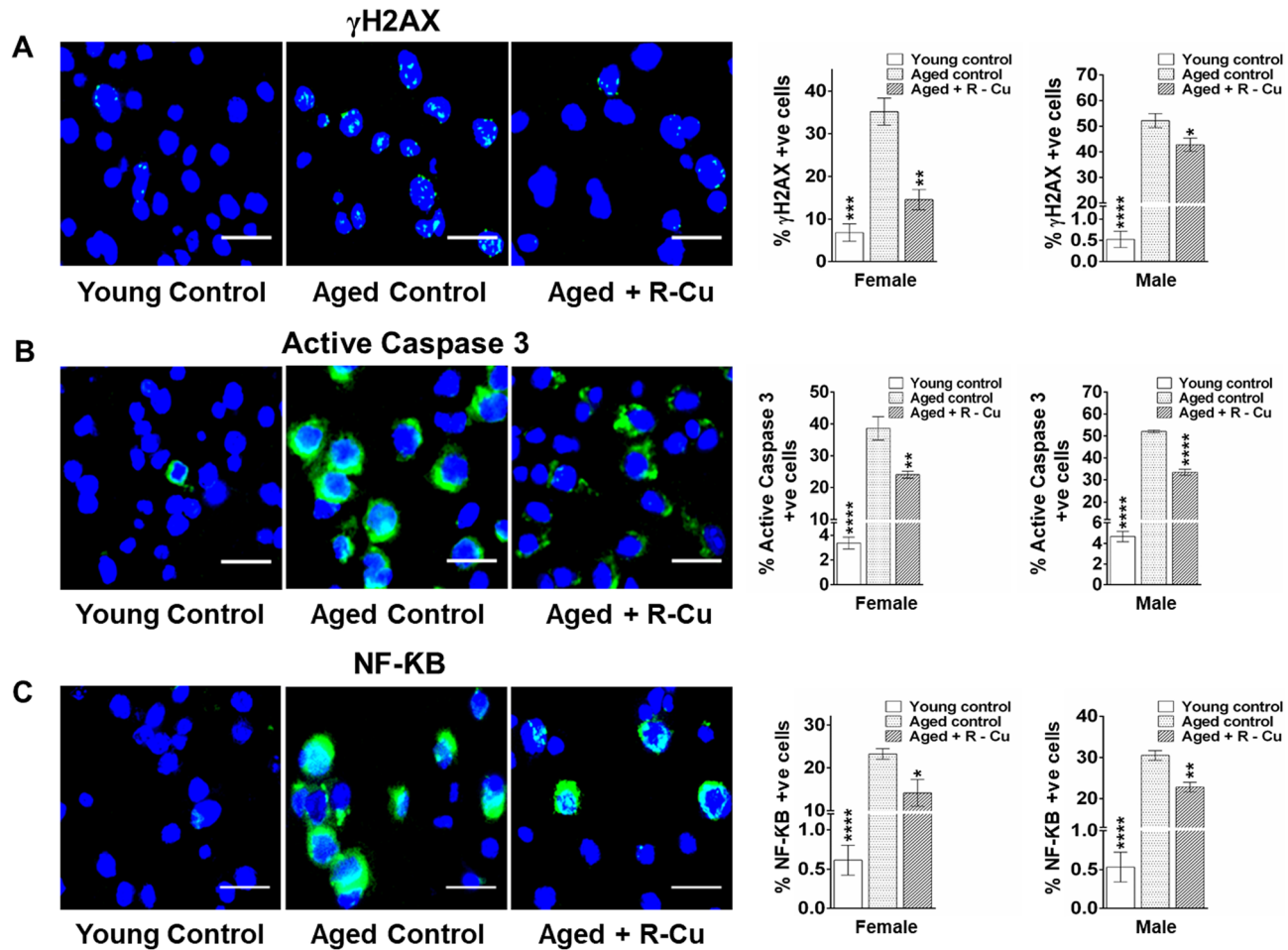


Figure 5. DNA damage, apoptosis and Inflammation in brain cells of ageing mice and their prevention by treatment with R-Cu. (A) Representative images of γ H2AX expression (Scale bar = 10 μ m) (left hand panel). Quantitative histograms (right hand panel). For each slide 1000 cells were analysed and percent cells positive for γ H2AX were calculated. Bars represent mean \pm SEM values. N = 4 animals in each group of both sexes. (B) Representative images of active caspase 3 expression (Scale bar = 10 μ m) (left hand panel). Quantitative histograms (right hand panel). For each slide 1000 cells were analysed and percent cells positive for caspase-3 were calculated. Bars represent mean \pm SEM values. N = 4 animals in each group of both sexes. (C) Representative images of NF- κ B expression (Scale bar = 10 μ m) (left hand panel). Quantitative histograms (right hand panel). For each slide 1000 cells were analysed and percent cells positive for NF- κ B were calculated. Bars represent mean \pm SEM values. N = 4 animals in each group of both sexes. For (A–C), levels in young controls and R-Cu treated ageing animals were compared with those of ageing controls, and statistical analysis was performed by two-tailed Student's t test. * p < 0.05; ** p < 0.01; *** p < 0.001; **** p < 0.0001.

we show in this article that prolonged oral administration of R-Cu to ageing mice down-regulated multiple biological hallmarks of ageing and neurodegeneration by virtue of its ability to deactivate cfChPs. Our results suggest that R-Cu may qualify as an ideal anti-ageing agent since it has the potential to simultaneously retard or delay the many conditions that are associated with ageing². To be globally applicable, an ideal anti-ageing agent should also be inexpensive and non-toxic—the two criteria that are also met by R-Cu. The latter can be easily administered orally, and both R and Cu are already approved for human use. An illustrated summary of the study design and the mechanisms by which R-Cu generated oxygen radicals eradicate cfChPs from brain micro-environment leading to down-regulation of ageing hallmarks is provided in Fig. 10.

The mechanism(s) by which R-Cu down-regulates the multiple biological hallmarks of ageing and neurodegeneration needs elaboration. Reversal of telomere shortening by R-Cu may suggest that telomere shortening could be a consequence of DNA damage inflicted by cfChPs which shear off telomere ends causing them to shorten. We observed differential effects between female and male mice with respect to telomere abnormalities. R-Cu effects in preventing telomere abnormalities in female mice were statistically significant for all parameters tested, while this was not the case in male mice. The biological explanation for this discrepant finding remains to be determined. Breakage of telomere ends may also help to explain our detection of persistent γ -H2AX signals in telomere regions of brain cells (DNA-SCARS)—an established signature of senescence⁴³. The bare chromosomal ends can fuse with each other to lead to chromosomal instability and aneuploidy⁴⁸, as was detected in our study.

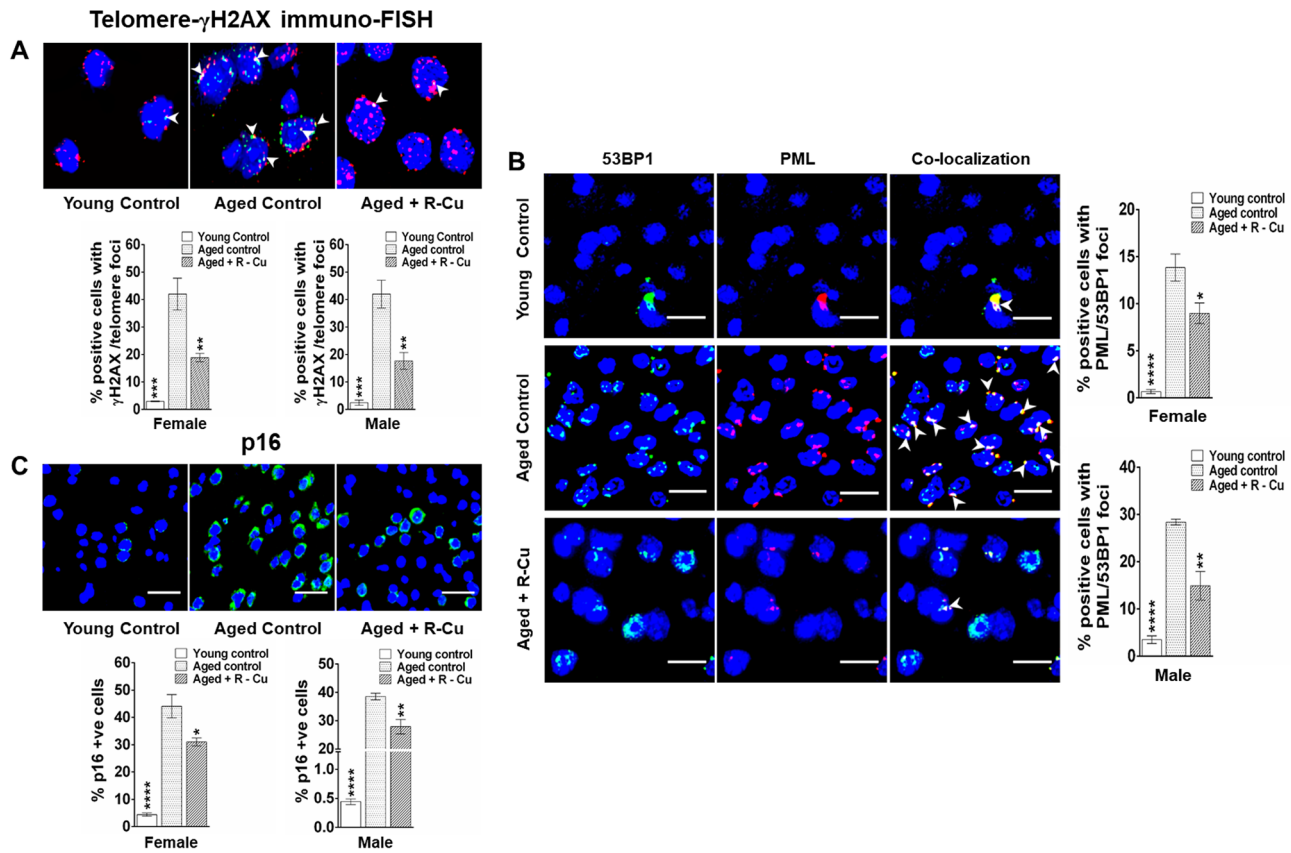


Figure 6. Activation of hallmarks of senescence in brain cells of ageing mice and their prevention by treatment with R-Cu. (A) Representative immuno-FISH images showing co-localization of fluorescent signals of γ -H2AX and telomeres (upper panel) (Scale bar = 10 μ m). Histograms of quantitative estimation of co-localised signals (lower panel). For each slide 500 nuclei were analysed and percent cells showing co-localisation of γ H2AX and telomere signals were calculated. Bars represent mean \pm SEM values. N = 4 animals in each group of both sexes. (B) Representative IF images showing co-localization of fluorescent signals of 53BP1 and PML (left hand panel) (Scale bar = 10 μ m). Histograms of quantitative estimation of co-localised signals (right hand panel). For each slide 500 nuclei were analysed and percent cells showing co-localisation of 53BP1 and PML signals were calculated. Bars represent mean \pm SEM values. N = 4 animals in each group of both sexes. (C) Representative images of p16 expression (upper panel) (Scale bar = 10 μ m) and quantitative histograms (lower panel). For each slide 1000 cells were analysed and percent cells positive for p16 was calculated. Bars represent mean \pm SEM values. N = 4 animals in each group of both sexes. In (A–C), values in young controls and R-Cu treated ageing animals were compared with those of ageing controls, and statistical analysis was performed by two-tailed Student's t test. * p < 0.05, ** p < 0.01; *** p < 0.001; **** p < 0.0001.

With respect to mitochondrial dysfunction, we have recently reported that internalised cfChPs, in addition to inflicting damage to genomic DNA, can inflict physical damage to mitochondria⁵⁸. One of the indicators of mitochondrial damage detected in that study was up-regulation of TOMM20⁵⁸. Our finding in the present study of TOMM20 over-expression in ageing mice, and its reversal by R-Cu is consistent with the possibility that mitochondrial damage in ageing mice is induced by cfChPs that are released from dying brain cells. However, reduction in amyloid plaque formation following prolonged R-Cu treatment would suggest an unknown role of cfChPs which calls for further research. Similarly, the mechanism(s) by which R-Cu reduced metabolic dysfunction in ageing mice leading to reduction in serum levels of glucose, cholesterol and CRP remains unknown at present. Taken together, it can be concluded that cfChPs have pleiotropic effects with wide ranging implications in ageing and neurodegeneration which remain open to future research.

We did not detect any evidence of damage to genomic DNA of brain cells that could be attributed to oxygen radicals that are generated following one year of R-Cu treatment. The markedly up-regulated antioxidant enzyme SOD in R-Cu treated mice apparently neutralised the invading oxygen radicals and prevented damage to cellular genomic DNA (vide Fig. 1). Thus, entry of R-Cu generated oxygen radicals into brain cells leads to up-regulation of SOD, which in turn protected the genome from ROS induced oxidative damage. This was further substantiated by our finding of a reduction in γ -H2AX signals in the post R-Cu treated mice (vide Fig. 5A). Overall, we observed no adverse effects in mice which had been administered R-Cu for a period of one year. This suggested that genomes of all cells of the body were similarly protected from the potentially damaging effects of oxygen radicals by up-regulated anti-oxidant enzymes.

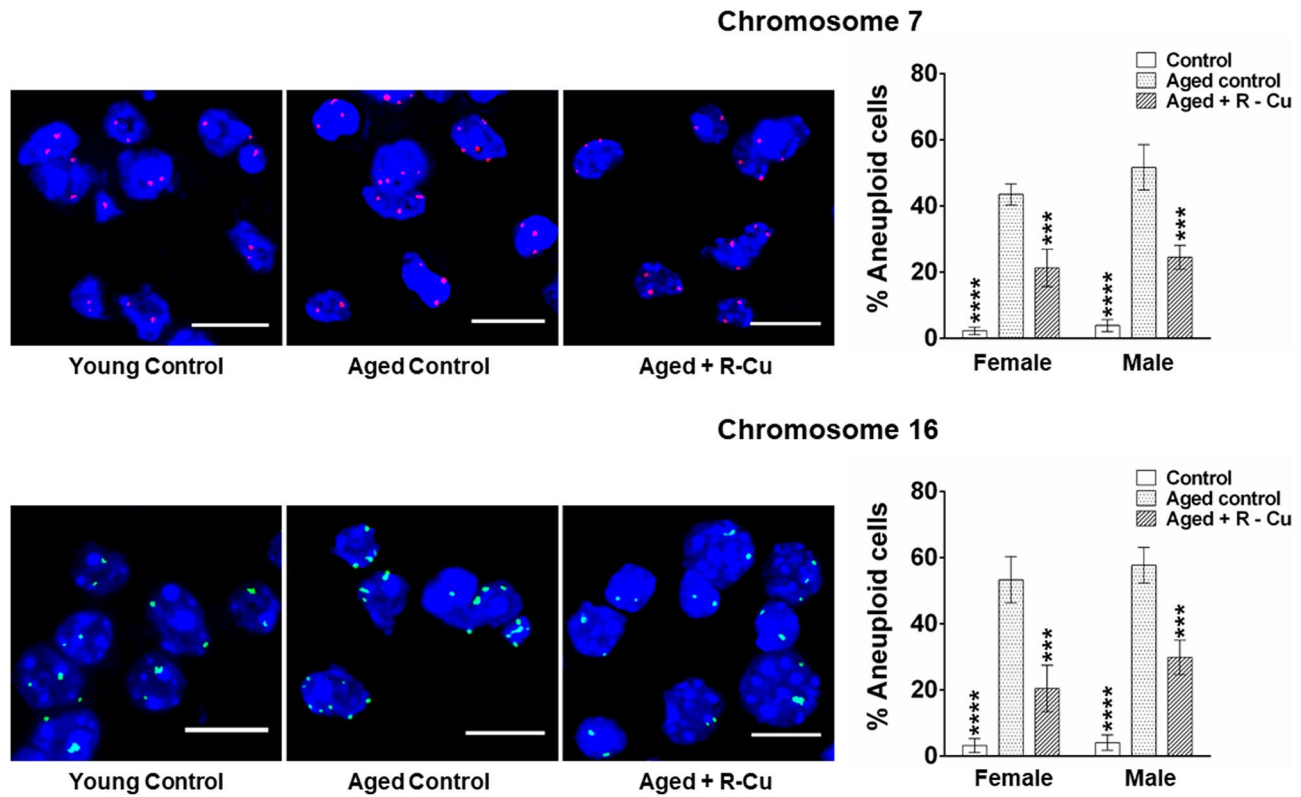


Figure 7. Development of aneuploidy in brain cells of ageing mice and its prevention by treatment with R-Cu. Representative images of aneuploidy of chromosome 7 and chromosome 16 in brain cells (left hand panels) (Scale bar = 10 μ m). Quantitative histograms representing percent aneuploid cells (right hand panels). Number of fluorescent signals per nucleus was counted, and signals less than 2 N or more than 2 N in a nucleus were taken as evidence of aneuploidy. Five fields (\sim 500 nuclei) were analysed and average number of signals per nucleus was calculated. Bars represent mean \pm SEM values. N = 4 animals in each group of both sexes. Values in young controls and R-Cu treated ageing animals were compared with those of ageing controls, and statistical analysis was performed by two-tailed Student's t test. *** p < 0.001; **** p < 0.0001.

Our study has some limitations. For example, it does not address the effects of R-Cu on physiological functions such as memory or behavioral aspects of the animals, or whether it extends survival. The effects of stopping exposure to R-Cu was also not investigated; whether the observed changes would revert or disappear remains unknown. The study also does not address whether the phenomenon of hormesis is involved in the biological effects that we observed^{59,60}. This issue is particularly relevant since we used low doses of R and Cu, both of which have been reported to exhibit hormetic effects^{61,62}. It has been reported that successful response to R therapy is due to its hormetic actions: exerting beneficial effects at low doses and cytotoxic effects at higher doses⁶¹. With respect to Cu, prior treatment of animals with low doses has been shown to protect them from higher lethal doses of Cu⁶². We do not provide direct evidence that admixing R with Cu leads to generation of oxygen radicals by virtue of the ability of R to reduce Cu(II) to Cu(I). Deactivation of cfChPs in extracellular spaces of brain that we observed assumes that this is effected by oxygen radicals; we do not actually demonstrate the presence of oxygen radicals in mouse brain. However, our finding of increased SOD activity in serum of R-Cu treated mice leads to the assumption that oxygen radicals might have also been generated in the brain. We also did not examine the mechanism by which oxygen radicals are absorbed from stomach or whether they were reactive against cfChPs. Finally, we observed that R-Cu treatment leads to increase in expression of SOD in brain cells. This does not necessarily imply increased SOD activity.

It is believed that ageing is a consequence of oxidative stress leading to progressive loss of tissue and organ function resulting from accumulation of ROS-induced damage^{63,64}. However, antioxidant therapy to retard ageing in animal models has produced conflicting results^{65,66}, and those in humans have been equivocal⁶⁷. Of all antioxidants, resveratrol has been the most widely investigated as an anti-ageing agent⁶⁸. Our current results raise the hypothesis that the reported anti-ageing effects of resveratrol may in fact be due to its pro-oxidant activity in the presence of copper. The conflicting results may reflect the inconsistent availability of copper in the stomach for resveratrol to have a sustained pro-oxidant activity in order to effectively deactivate extra-cellular cfChPs and to have a protective effect against ageing.

We demonstrate for the first time that cfChPs derived from dying brain cells are abundantly present in the extracellular spaces of the ageing brain. We also show that extra-cellular cfChPs are virtually eliminated by oxygen radicals that are generated following prolonged treatment with R-Cu. The fact that elimination of cfChPs was associated with down-regulation of multiple biological hallmarks of ageing and neurodegeneration makes a strong case for a direct role of cfChPs in the aetiology of these pathological processes. We propose that cfChPs

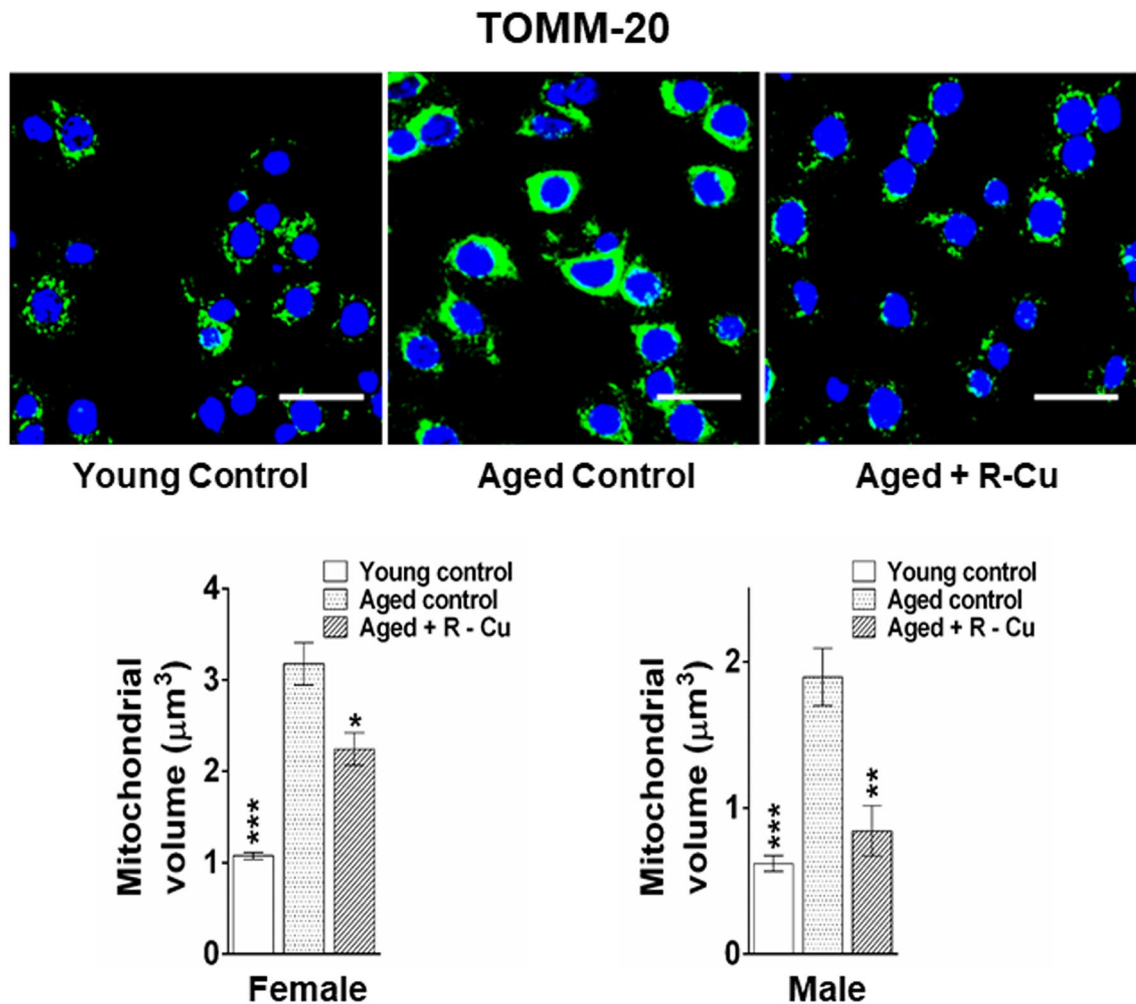


Figure 8. Increased mitochondrial dysfunction in ageing mice and its prevention by treatment with R-Cu. Representative IF images showing expression of TOMM20 (upper panel) (Scale bar = 10 μm). Quantitative histograms representing mitochondrial volume changes (lower panel). Five fields (~ 2000 mitochondria) were analysed and average volumetric change was estimated using IMARIS software 7.2.3 (<http://www.bitplane.com>, Bitplane Technologies, AG). Bars represent mean \pm SEM values. N = 4 animals in each group of both sexes. Values in young controls and R-Cu treated ageing animals were compared with those of ageing controls, and statistical analysis was performed by two-tailed Student's t test. * $p < 0.05$; ** $p < 0.01$; *** $p < 0.001$.

released from dying brain cells initiate a vicious cycle of more DNA damage, apoptosis and inflammation, setting in motion a low grade and unrelenting “cytokine storm”⁶⁹. We propose that the latter, together with other yet unknown harmful pleiotropic effects of cfChPs, are the underlying processes that define ageing. Our results suggest that these harmful effects can be prevented by deactivation/eradication of the offending cfChPs via the medium of oxygen radicals. We propose that oral administration of a combination of small quantities of R and Cu holds the promise of being an effective anti-ageing therapeutic combination. Whether R-Cu will be effective in retarding ageing and neurodegeneration in humans will have to await clinical trials in appropriate populations. It is to be noted in this context that our early results have shown that R-Cu is therapeutically effective in humans, albeit in relation to other pathological situations^{26,27}.

Over the past fifty years of biogerontological research, many theories and causes of ageing have been advanced^{9,10}, but none can comprehensively explain the myriad changes that accompany this multidimensional process. While we acknowledge that there may be other factors at play, our results suggest that cfChPs may be global instigators of ageing and neurodegeneration, and that therapeutic use of R-Cu may help to make healthy ageing an attainable goal.

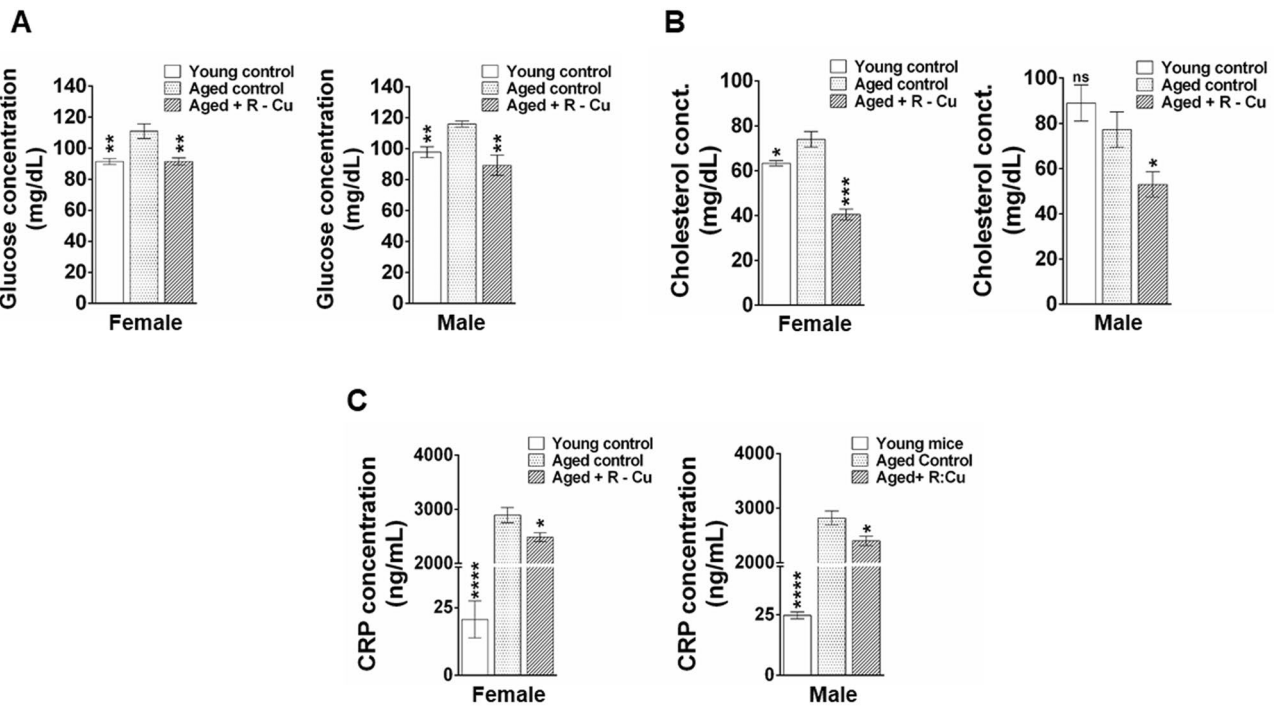
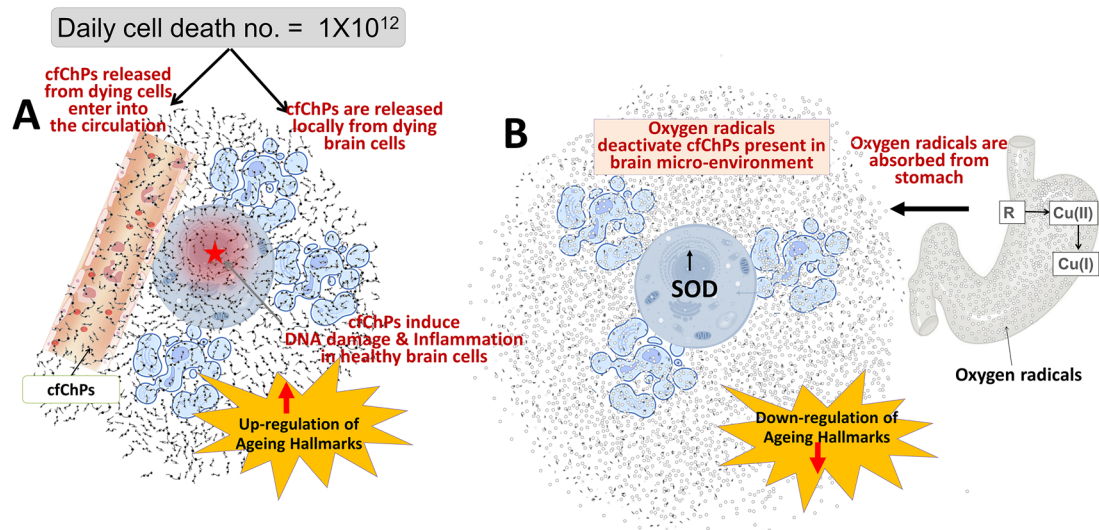


Figure 9. Increased metabolic dysfunction in ageing mice and their prevention by treatment with R-Cu. (A–C) represent histograms of levels of serum glucose, cholesterol and CRP, respectively. Bars represent mean \pm SEM values. N = 4 animals in each group of both sexes except in cholesterol female young control (N = 3) and cholesterol male young control (N = 2). Levels in young controls and R-Cu treated ageing animals were compared with those of ageing controls, and statistical analysis was performed by two-tailed Student's t test. *p < 0.05; **p < 0.01; ***p < 0.001; ****p < 0.0001.

Study design



Mechanism



Ageing hallmarks modulation

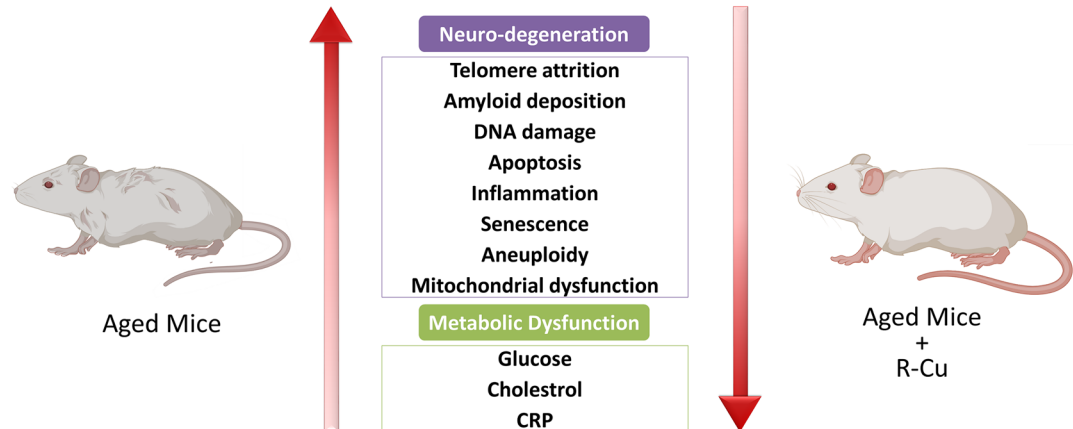


Figure 10. Graphical illustration of the study design and the mechanisms involved in oxygen radical induced down-regulation of biological hallmarks in ageing in brain cells following R-Cu treatment. (A) cfChPs that diffuse out from circulation, or those that are released locally from dying brain cells, are readily internalised by healthy brain cells, wherein they activate multiple biological hallmarks of ageing. (B) Oxygen radicals are generated in the stomach upon oral administration of R-Cu which are readily absorbed leading to systemic effects in the form of deactivation/eradication of cfChPs in the brain micro-environment. Deactivation/eradication of cfChPs leads to down-regulation of biological hallmarks of ageing in brain cells. Oxygen radicals also enter into the healthy brain cells; but their entry leads to activation of the anti-oxidant enzyme superoxide dismutase (SOD), which detoxifies and eliminates the offending agents, thereby protecting the genomic DNA.

Data availability

All data relevant to interpretation of the results are self-contained within the manuscript. Raw data can be found at Figshare dataset repository (<https://doi.org/10.6084/m9.figshare.20265906>).

Received: 30 June 2022; Accepted: 27 September 2022

Published online: 14 October 2022

References

1. Ghebreyesus, T. A. It takes knowledge to transform the world to be a better place to grow older. *Nat. Aging* **1**, 865–865 (2021).
2. Bellantuono, I. Find Drugs that delay many diseases of old age. *Nature* **554**, 293–295 (2018).
3. Kaeberlein, M., Rabinovitch, P. S. & Martin, G. M. Healthy aging: The ultimate preventative medicine. *Science* **350**, 1191–1193 (2015).
4. López-Otín, C., Blasco, M. A., Partridge, L., Serrano, M. & Kroemer, G. The Hallmarks of aging. *Cell* **153**, 1194–1217 (2013).
5. Xia, X., Jiang, Q., McDermott, J. & Han, J.-D.J. Aging and Alzheimer's disease: Comparison and associations from molecular to system level. *Aging Cell* **17**, e12802 (2018).
6. Chio, Y. A., Lakatta, E., Ungvari, Z., Dai, D.-F. & Rabinovitch, P. Cardiovascular disease and aging. *Adv. Gerosci.* https://doi.org/10.1007/978-3-319-23246-1_5 (2016).
7. Kalyani, R. R., Golden, S. H. & Cefalu, W. T. Diabetes and aging: Unique considerations and goals of care. *Diabetes Care* **40**, 440–443 (2017).
8. Aunan, J. R., Cho, W. C. & Søreide, K. The biology of aging and cancer: A brief overview of shared and divergent molecular hallmarks. *Aging Dis.* **8**, 628–642 (2017).
9. da Costa, J. P. *et al.* A synopsis on aging—Theories, mechanisms and future prospects. *Ageing Res. Rev.* **29**, 90–112 (2016).
10. Jin, K. Modern biological theories of aging. *Aging Dis.* **1**, 72–74 (2010).
11. Schumacher, B., Pothof, J., Vijg, J. & Hoeijmakers, J. H. J. The central role of DNA damage in the ageing process. *Nature* **592**, 695–703 (2021).
12. Ferrucci, L. & Fabbri, E. Inflammageing: chronic inflammation in ageing, cardiovascular disease, and frailty. *Nat Rev Cardiol.* **15**, 505–522 (2018).
13. Mittra, I. *et al.* Circulating nucleic acids damage DNA of healthy cells by integrating into their genomes. *J. Biosci.* **40**, 91–111 (2015).
14. Mittra, I. *et al.* Cell-free chromatin from dying cancer cells integrate into genomes of bystander healthy cells to induce DNA damage and inflammation. *Cell Death Discov.* **3**, 1–14 (2017).
15. Raghuram, G. V., Chaudhary, S., Johari, S. & Mittra, I. Illegitimate and repeated genomic integration of cell-free chromatin in the aetiology of somatic mosaicism, ageing, chronic diseases and cancer. *Genes (Basel)* **10**, 1–19 (2019).
16. Tripathy, B. K., Pal, K., Shabirish, S. & Mittra, I. A new perspective on the origin of DNA double-strand breaks and its implications for ageing. *Genes (Basel)* **12**, 1–12 (2021).
17. Mittra, I., Nair, N. K. & Mishra, P. K. Nucleic acids in circulation: Are they harmful to the host?. *J. Biosci.* **37**, 301–312 (2012).
18. Mittra, I. *et al.* Prevention of chemotherapy toxicity by agents that neutralize or degrade cell-free chromatin. *Ann. Oncol.* **28**, 2119–2127 (2017).
19. Kirolikar, S. *et al.* Prevention of radiation-induced bystander effects by agents that inactivate cell-free chromatin released from irradiated dying cells. *Cell Death Dis.* **9**, 1–16 (2018).
20. Mittra, I. *et al.* Cell-free chromatin particles released from dying host cells are global instigators of endotoxin sepsis in mice. *PLoS ONE* **15**, 1–22 (2020).
21. Diaz-Gerevini, G. T. *et al.* Beneficial action of resveratrol: How and why?. *Nutrition* **32**, 174–178 (2016).
22. Bost, M. *et al.* Dietary copper and human health: Current evidence and unresolved issues. *J. Trace Elem. Med. Biol.* **35**, 107–115 (2016).
23. Fukuhara, K. & Miyata, N. Resveratrol as a new type of DNA-cleaving agent. *Bioorg. Med. Chem. Lett.* **8**, 3187–3192 (1998).
24. Fukuhara, K. *et al.* Structural basis for DNA-cleaving activity of resveratrol in the presence of Cu(II). *Bioorg. Med. Chem.* **14**, 1437–1443 (2006).
25. Subramanian, S., Vohra, I., Iyer, A., Nair, N. K. & Mittra, I. A paradoxical synergism between resveratrol and copper (II) with respect to degradation of DNA and RNA [version2; referees: 2 approved]. *F1000Research* **4**, 1145 (2015).
26. Mittra, I. *et al.* Resveratrol and Copper for treatment of severe COVID-19: an observational study (RESCU 002). *medRxiv* **6**, 1–13 (2020).
27. Agarwal, A. *et al.* A novel pro-oxidant combination of resveratrol and copper reduces transplant related toxicities in patients receiving high dose melphalan for multiple myeloma (RESCU 001). *PLoS ONE* **17**, 1–9 (2022).
28. Wang, T. *et al.* Copper supplementation reverses dietary iron overload-induced pathologies in mice. *J. Nutr. Biochem.* **59**, 56–63 (2018).
29. Baur, J. A. *et al.* Resveratrol improves health and survival of mice on a high-Calorie Diet. *Nature* **444**, 337–342 (2006).
30. Callicott, R. J. & Womack, J. E. Real-time PCR assay for measurement of mouse telomeres. *Comp. Med.* **56**, 17–22 (2006).
31. Cawthon, R. M. Telomere measurement by quantitative PCR. *Nucleic Acids Res.* **30**, 1–6 (2002).
32. Blackburn, E. H., Epel, E. S. & Lin, J. Human telomere biology: A contributory and interactive factor in aging, disease risks, and protection. *Science* **350**, 1193–1198 (2015).
33. Raz, V. *et al.* The nuclear lamina promotes telomere aggregation and centromere peripheral localization during senescence of human mesenchymal stem cells. *J. Cell Sci.* **121**, 4018–4028 (2008).
34. Rodriguez, K. M. *et al.* β -Amyloid burden in healthy aging. *Neurology* **78**, 387–395 (2012).
35. Murphy, M. P. & Levine, H. Alzheimer's disease and the amyloid- β peptide. *J. Alzheimer's Dis.* **19**, 311–323 (2010).
36. Erickson, K. I. *et al.* Brain-derived neurotrophic factor is associated with age-related decline in hippocampal volume. *J. Neurosci.* **30**, 5368–5375 (2010).
37. White, R. R. & Vijg, J. Do DNA double-strand breaks drive aging?. *Mol Cell* **63**, 729–738 (2016).
38. Zhang, Y. & Herman, B. Ageing and apoptosis. *Mech. Ageing Dev.* **123**, 245–260 (2002).
39. Chung, H. Y. *et al.* Redefining chronic inflammation in aging and age-related diseases: Proposal of the senoinflammation concept. *Aging Dis.* **10**, 367–382 (2019).
40. Rogakou, E. P., Pilch, D. R., Orr, A. H., Ivanova, V. S. & Bonner, W. M. DNA double-stranded breaks induce histone H2AX phosphorylation on serine 139. *J. Biol. Chem.* **273**, 5858–5868 (1998).
41. Porter, A. G. & Jänicke, R. U. Emerging roles of caspase-3 in apoptosis. *Cell Death Differ.* **6**, 99–104 (1999).
42. Micco, R. Di, Krizhanovsky, V., Baker, D. & Fagagna, F. d'Adda di. Cellular senescence in ageing: from mechanisms to therapeutic opportunities. *Nat. Rev. Mol. Cell Biol.* **22**, 75–95 (2021).
43. Rodier, F. *et al.* DNA-SCARS: Distinct nuclear structures that sustain damage-induced senescence growth arrest and inflammatory cytokine secretion. *J. Cell Sci.* **124**, 68–81 (2011).
44. Narita, M. Cellular senescence and chromatin organisation. *Br. J. Cancer* **96**, 686–691 (2007).
45. Bischof, O. *et al.* Deconstructing PML-induced premature senescence. *EMBO J.* **21**, 3358–3369 (2002).

46. Mirza-Aghazadeh-Attari, M. *et al.* 53BP1: A key player of DNA damage response with critical functions in cancer. *DNA Repair (Amst.)* **73**, 110–119 (2019).
47. Baker, D. J. *et al.* Naturally occurring p16Ink4a -positive cells shorten healthy lifespan. *Nature* **530**, 184–189 (2016).
48. Naylor, R. M. & van Deursen, J. M. Aneuploidy in cancer and aging Ryan. *Annu. Rev. Genet.* **50**, 45–66 (2016).
49. Sun, N., Youle, R. J. & Finkel, T. The mitochondrial basis of aging. *Mol. Cell* **61**, 654–666 (2016).
50. Chacinska, A., Koehler, C. M., Milenkovic, D., Lithgow, T. & Pfanner, N. Importing mitochondrial proteins: Machineries and mechanisms. *Cell* **138**, 628–644 (2009).
51. Leiter, L. A. *et al.* Postprandial glucose regulation: New data and new implications. *Clin. Ther.* **27**, S42–S56 (2005).
52. Félix-Redondo, F. J., Grau, M. & Fernández-Bergés, D. Cholesterol and cardiovascular disease in the elderly. Facts and gaps. *Aging Dis.* **4**, 154–169 (2013).
53. Leiter, E. H., Premdas, F., Harrison, D. E. & Lipson, L. G. Aging and glucose homeostasis in C57BL/6J male mice. *FASEB J.* **2**, 2807–2811 (1988).
54. Halliwell, B. & Gutteridge, J. M. C. Role of free radicals and catalytic metal ions in human disease: An overview. *Methods Enzymol.* **186**, 1–85 (1990).
55. Pizzino, G. *et al.* Oxidative stress: Harms and benefits for human health. *Oxid. Med. Cell. Longev.* **2017**, 1–13 (2017).
56. Fliedner, T. M., Graessle, D., Paulsen, C. & Reimers, K. Structure and function of bone marrow hemopoiesis: Mechanisms of response to ionizing radiation exposure. *Cancer Biother. Radiopharm.* **17**, 405–426 (2002).
57. Sender, R. & Milo, R. The distribution of cellular turnover in the human body. *Nat. Med.* **27**, 45–48 (2021).
58. Tripathy, B. K. *et al.* Cell-free chromatin particles released from dying cells inflict mitochondrial damage and ROS production in living cells. *bioRxiv* <https://doi.org/10.1101/2021.12.30.474529> (2021).
59. Calabrese, E. J. & Mattson, M. P. How does hormesis impact biology, toxicology, and medicine?. *NPJ Aging Mech. Dis.* **3**(1), 1–8 (2017).
60. Rattan, S. I. Physiological hormesis and hormetins in biogerontology. *Curr. Opin. Toxicol.* (2022).
61. Petrovski, G., Gurusamy, N. & Das, D. K. Resveratrol in cardiovascular health and disease. *Ann. N. Y. Acad. Sci.* **1215**(1), 22–33 (2011).
62. Bozhkov, A. I., Sidorov, V. I., Kurguzova, N. I. & Dlubovskaya, V. L. Metabolic memory enhances hormesis effect to the copper ions in age-dependent manner. *Adv. Gerontol. = Uspekhi Gerontologii* **27**(1), 72–80 (2014).
63. Harman, D. Aging: A theory based on free radical and radiation chemistry. *J. Gerontol.* **11**, 298–300 (1956).
64. Finkel, T. & Holbrook, N. J. Oxidants, oxidative stress and the biology of ageing. *Nature* **408**, 239–247 (2000).
65. Hamilton, R. T., Walsh, M. E. & Van Remmen, H. Mouse models of oxidative stress indicate a role for modulating healthy aging. *J. Clin. Exp. Pathol.* **01**, 1–30 (2012).
66. Zhou, D. D. *et al.* Effects and Mechanisms of Resveratrol on Aging and Age-Related Diseases. *Oxid. Med. Cell. Longev.* **2021**, (2021).
67. Fusco, D., Colloca, G., Lo Monaco, M. R. & Cesari, M. Effects of antioxidant supplementation on the aging process. *Clin. Interv. Aging* **2**, 377–387 (2007).
68. Pyo, I. S., Yun, S., Yoon, Y. E., Choi, J. W. & Lee, S. J. Mechanisms of aging and the preventive effects of resveratrol on age-related diseases. *Molecules* **25**, (2020).
69. Shabrish, S. & Mittra, I. Cytokine storm as a cellular response to dsDNA breaks: A new proposal. *Front. Immunol.* **12**, 1–10 (2021).

Acknowledgements

We sincerely thank Dr. Snehal Shabrish for preparing the info graphic and Mr. Roshan Shaikh and Mr. Ashish Pawar for their help in preparing the manuscript.

Author contributions

K.P., G.V.R., J.D., S.S., V.J., A.S., B.R., H.T., D.K. and S.C. conducted the experiment. I.M., K.P. and G.V.R supervised the experiments. K.P. and G.V.R conducted data analysis. I.M. conceptualized the project, was responsible for overall supervision and procured funding. I.M., K.P. and G.V.R. wrote the paper. I.M. approved the final manuscript.

Funding

This study was supported by the Department of Atomic Energy, Government of India, through its grant CTCTMC to Tata Memorial Centre awarded to IM. The funding agency had no role in research design, collection, analysis, and interpretation of data and manuscript writing.

Competing interests

The authors declare no competing interests.

Additional information

Supplementary Information The online version contains supplementary material available at <https://doi.org/10.1038/s41598-022-21388-w>.

Correspondence and requests for materials should be addressed to I.M.

Reprints and permissions information is available at www.nature.com/reprints.

Publisher's note Springer Nature remains neutral with regard to jurisdictional claims in published maps and institutional affiliations.



Open Access This article is licensed under a Creative Commons Attribution 4.0 International License, which permits use, sharing, adaptation, distribution and reproduction in any medium or format, as long as you give appropriate credit to the original author(s) and the source, provide a link to the Creative Commons licence, and indicate if changes were made. The images or other third party material in this article are included in the article's Creative Commons licence, unless indicated otherwise in a credit line to the material. If material is not included in the article's Creative Commons licence and your intended use is not permitted by statutory regulation or exceeds the permitted use, you will need to obtain permission directly from the copyright holder. To view a copy of this licence, visit <http://creativecommons.org/licenses/by/4.0/>.

© The Author(s) 2022